

Non Gaussian extrema counts for CMB maps

Dmitri Pogosyan¹, Christophe Pichon², and Christophe Gay²

¹ *Department of Physics, University of Alberta, 11322-89 Avenue, Edmonton, Alberta, T6G 2G7, Canada*

² *Institut d'astrophysique de Paris, 98, bis boulevard Arago, 75 014, Paris, France*

In the context of the geometrical analysis of weakly non Gaussian CMB maps, the 2D differential extrema counts as functions of the excursion set threshold is derived from the full moments expansion of the joint probability distribution of an isotropic random field, its gradient and invariants of the Hessian. Analytic expressions for these counts are given to second order in the non Gaussian correction, while a Monte Carlo method to compute them to arbitrary order is presented. Matching count statistics to these estimators is illustrated on fiducial non Gaussian ‘‘Planck’’ data.

PACS numbers: 98.80.Jk,98.70.Vc,98.65.Dx,02.50.Sk

Random fields are ubiquitous phenomena in physics appearing in areas ranging from turbulence to the landscape of string theories. In cosmology, the sky-maps of the polarized Cosmic Microwave Background (CMB) radiation – a focal topic of current research – is a prime example of such 2D random fields. Modern view of the cosmos, developed primarily through statistical analysis of these fields, points to a Universe that is statistically homogeneous and isotropic with a hierarchy of structures arising from small Gaussian fluctuations of quantum origin. While the Gaussian limit provides the fundamental starting point in the study of random fields [1–3], non-Gaussian features of the CMB fields are of great interest. Indeed, CMB inherits a high level of gaussianity from initial fluctuations, but small non-Gaussian deviations may provide a unique window into the details of processes in the early Universe. The search for the best methods to analyze non-Gaussian random fields is ongoing.

In paper [4] the general invariant based formalism for computing topological and geometrical characteristics of non Gaussian fields was presented. The general formulae for the Euler characteristics to all orders has been derived, which encompasses the well known first correction [5] and which was later confirmed to the next order by [6]. We now focus on the statistics of the density of extremal points which follows directly from the formalism of [4]. The goal of this paper is to provide an explicit recipe on how to use this formalism in practice on idealised 2D CMB ‘‘Planck’’-like data.

I. EXTREMA COUNTS

Extrema counts, especially that of the maxima of the field, have long application to cosmology [e.g. 3], however theoretical development have been mostly restricted to the Gaussian fields. The statistics of extrema counts, as well as of the Euler number, requires the knowledge

of the one-point joint probability distribution function (JPDF) $P(x, x_i, x_{ij})$ of the field x , its first, x_i , and second, x_{ij} , derivatives [12]. Extrema density is an intrinsically isotropic statistics given by [1, 7]

$$\frac{\partial n_{\text{ext}}}{\partial x} = \int d^3x_{ij} P(x, x_i = 0, x_{ij}) |x_{ij}|. \quad (1)$$

Under the condition of statistical isotropy of the field, the essential form for the JPDF is therefore given in terms of the rotation invariants – x itself, the square of the magnitude of the gradient $q^2 \equiv x_1^2 + x_2^2$ and the two invariants $J_1 \equiv \lambda_1 + \lambda_2$, $J_2 \equiv (\lambda_1 - \lambda_2)^2$ of the Hessian matrix x_{ij} (where λ_i are the eigenvalues of the Hessian). Introducing $\zeta = (x + \gamma J_1)/\sqrt{1 - \gamma^2}$ (where the spectral parameter $\gamma = -\langle x J_1 \rangle$ characterizes the shape of the underlying power spectrum), leads to the following JPDF for the Gaussian 2D field

$$G_{2D} = \frac{1}{2\pi} \exp \left[-\frac{1}{2} \zeta^2 - q^2 - \frac{1}{2} J_1^2 - J_2 \right]. \quad (2)$$

The invariant form for the extrema counts

$$\frac{\partial n_{\text{ext}}}{\partial x} = \int \frac{dJ_1 dJ_2}{8\pi^2 \sqrt{1 - \gamma^2}} \exp \left[-\frac{1}{2} \zeta^2 - \frac{1}{2} J_1^2 - J_2 \right] |J_1^2 - J_2|$$

then readily recovers the classical results [1, 3, 7] when the limits of integration that define the extrema type are implemented, namely $J_1 \in [-\infty, 0]$, $J_2 \in [0, J_1^2]$ for maxima, $J_1 \in [0, \infty]$, $J_2 \in [0, J_1^2]$ for minima and $J_1 \in [-\infty, \infty]$, $J_2 \in [J_1^2, \infty]$ for saddle points.

In [4] we have observed that for non-Gaussian JPDF the invariant approach immediately suggests a Gram-Charlier expansion in terms of the orthogonal polynomials defined by the kernel G_{2D} . Since ζ , q^2 , J_1 and J_2 are uncorrelated variables in the Gaussian limit, the resulting expansion is

$$P_{2D}(\zeta, q^2, J_1, J_2) = G_{2D} \left[1 + \sum_{n=3}^{\infty} \sum_{i,j,k,l=0}^{i+2j+k+2l=n} \frac{(-1)^{j+l}}{i! j! k! l!} \left\langle \zeta^i q^{2j} J_1^k J_2^l \right\rangle_{\text{GC}} H_i(\zeta) L_j(q^2) H_k(J_1) L_l(J_2) \right], \quad (3)$$

where terms are sorted in the order of the field power n and $\sum_{i,j,k,l=0}^{i+2j+k+2l=n}$ stands for summation over all combinations of non-negative i, j, k, l such that $i + 2j + k + 2l$ adds to the order of the expansion term n . H_i are (*probabilists'*) Hermite and L_j are Laguerre polynomials.

The Gram-Charlier coefficients, $\left\langle \zeta^i q^{2j} J_1^k J_2^l \right\rangle_{\text{GC}} \equiv (-1)^{j+l} j! l! \left\langle H_i(\zeta) L_j(q^2) H_k(J_1) L_l(J_2) \right\rangle_{\text{m}}$ that appear in the expansion can be related to the more familiar cumulants of the field and its derivatives (we use $\langle \rangle_{\text{m}}$ for statistical moments while reserving $\langle \rangle$ for statistical cumulants), actually being identical to them for the first three orders $n = 3, 4, 5$. Lookup tables of the relationship between Gram-Charlier cumulants and statistical cumulants can be found at <http://www.iap.fr/users/pichon/Gram/>. As an illustration, one sixth order non trivial cumulant would be $\langle J_1^3 J_2 \zeta \rangle_{\text{CG}} = \langle J_1^3 J_2 \zeta \rangle + \langle J_1^3 \rangle \langle J_2 \zeta \rangle + 3 \langle J_1 J_2 \rangle \langle J_1^2 \zeta \rangle$. It is prudent to stress that the Gram-Charlier series expansion is distinct from the perturbative expansions. For instance, while the linear Edgeworth or f_{NL} expansion match solely to the first order $n = 3$ Gram-Charlier coefficients, quadratic terms require knowledge of the Gram-Charlier terms to $n = 6$, while the cubic ones to $n = 9$.

Integrals over J_1 and J_2 for extremal points can be carried out analytically even for the general expression (3). Different types of critical points can be evaluated separately by restraining the integration domain in the J_1 - J_2 plane to ensure the appropriate signs for the eigenvalues.

The effect of the non-Gaussian cubic correction on the total number of the extrema of different types is given by

$$n_{\text{max/min}} = \frac{1}{8\sqrt{3}\pi R_*^2} \pm \frac{18 \langle q^2 J_1 \rangle - 5 \langle J_1^3 \rangle + 6 \langle J_1 J_2 \rangle}{54\pi\sqrt{2}\pi R_*^2},$$

$$n_{\text{sad}} = \frac{1}{4\sqrt{3}\pi R_*^2}, \quad (4)$$

where we have restored (see note [11]) the dimensional scaling with $R_* = \sigma_1/\sigma_2$, the characteristic separation scale between extrema. The total number of saddles, as well as of all the extremal points, $n_{\text{max}} + n_{\text{min}} + n_{\text{sad}}$, are preserved in the first order (the latter following for the former, as topological considerations imply $n_{\text{max}} - n_{\text{sad}} + n_{\text{min}} = \text{const}$), but the symmetry between the minima and the maxima is broken.

The differential number counts with respect to the excursion threshold ν are given by

$$\frac{\partial n_{\text{max/min}}}{\partial \nu} = \frac{1}{\sqrt{2\pi} R_*^2} \exp\left(-\frac{\nu^2}{2}\right) \left[1 \pm \text{erf}\left(\frac{\gamma \nu}{\sqrt{2(1-\gamma^2)}}\right) \right] K_1(\nu, \gamma) \pm \frac{1}{\sqrt{2\pi(1-\gamma^2)} R_*^2} \exp\left(-\frac{\nu^2}{2(1-\gamma^2)}\right) K_3(\nu, \gamma)$$

$$+ \frac{\sqrt{3}}{\sqrt{2\pi(3-2\gamma^2)} R_*^2} \exp\left(-\frac{3\nu^2}{6-4\gamma^2}\right) \left[1 \pm \text{erf}\left(\frac{\gamma \nu}{\sqrt{2(1-\gamma^2)(3-2\gamma^2)}}\right) \right] K_2(\nu, \gamma), \quad (5)$$

$$\frac{\partial n_{\text{sad}}}{\partial \nu} = \frac{2\sqrt{3}}{\sqrt{2\pi(3-2\gamma^2)} R_*^2} \exp\left(-\frac{3\nu^2}{6-4\gamma^2}\right) K_2(\nu, \gamma), \quad (6)$$

where K_1, K_2, K_3 are polynomials with coefficients expressed in terms of the cumulants. Here we give explicit expressions for the first non-Gaussian order, while the next order can be found at the above mentioned URL.

The term $K_1(\nu, \gamma)$ has a special role determining the Euler number $\chi(\nu)$ via $\partial\chi/\partial\nu = \partial/\partial\nu (n_{\text{max}} + n_{\text{min}} - n_{\text{sad}}) = \sqrt{2/\pi} \exp(-\nu^2/2) K_1(\nu, \gamma)$. As such, its full expansion has been given in [4], Eq. (7), and confirmed to the second order in [6]. To the leading non-Gaussian order

$$K_1 = \frac{\gamma^2}{8\pi} \left[H_2(\nu) + \left(\frac{2}{\gamma} \langle q^2 J_1 \rangle + \frac{1}{\gamma^2} \langle x J_1^2 \rangle - \frac{1}{\gamma^2} \langle x J_2 \rangle \right) H_1(\nu) - \left(\langle x q^2 \rangle + \frac{1}{\gamma} \langle x^2 J_1 \rangle \right) H_3(\nu) + \frac{1}{6} \langle x^3 \rangle H_5(\nu) \right]. \quad (7)$$

Introducing scaled Hermite polynomials $\mathcal{H}_n^\pm(\nu, \sigma) \equiv \sigma^{\pm n} H_n(\nu/\sigma)$, the polynomial $K_2(\nu, \gamma)$, the only one that determines the distribution of saddle points, can be written as

$$K_2 = \frac{1}{8\pi\sqrt{3}} \left[1 - \left(\langle x q^2 \rangle + \frac{1}{3} \langle x J_1^2 \rangle - \frac{4}{3} \langle x J_2 \rangle + \frac{2}{3} \gamma \langle q^2 J_1 \rangle + \frac{2}{9} \gamma \langle J_1^3 \rangle - \frac{2}{3} \gamma \langle J_1 J_2 \rangle \right) \mathcal{H}_1^-(\nu, \sqrt{1-2/3\gamma^2}) \right. \\ \left. + \frac{1}{6} \left(\langle x^3 \rangle + 2\gamma \langle x^2 J_1 \rangle + \frac{4}{3} \gamma^2 \langle x J_1^2 \rangle + \frac{2}{3} \gamma^2 \langle x J_2 \rangle + \frac{8}{27} \gamma^3 \langle J_1^3 \rangle + \frac{4}{9} \gamma^3 \langle J_1 J_2 \rangle \right) \mathcal{H}_3^-(\nu, \sqrt{1-2/3\gamma^2}) \right]. \quad (8)$$

The remaining term, $K_3(\nu, \gamma)$ is the most complicated one. It is expressed as the expansion in $\mathcal{H}_n^+(\nu, \sqrt{1-\gamma^2})$:

$$\begin{aligned}
K_3 = & \frac{(1-\gamma^2)}{2(2\pi)^{3/2}(3-2\gamma^2)^3} \left[\gamma(3-2\gamma^2)^3 \mathcal{H}_1^+(\nu, \sqrt{1-\gamma^2}) + \left(\frac{1}{2} \gamma^3 (1+\gamma^2-26\gamma^4+28\gamma^6-8\gamma^8) \langle x^3 \rangle \right. \right. \\
& - \gamma^4 (26-28\gamma^2+8\gamma^4) \langle x^2 J_1 \rangle + \gamma (1-\gamma^2) (1+2\gamma^2) (3-2\gamma^2)^2 \langle x q^2 \rangle - \gamma (24-26\gamma^2+8\gamma^4) \langle x J_1^2 \rangle \\
& + \gamma (15-23\gamma^2+8\gamma^4) \langle x J_2 \rangle + 4(1-\gamma^2) (3-2\gamma^2)^2 \langle q^2 J_1 \rangle - (10-12\gamma^2+4\gamma^4) \langle J_1^3 \rangle + 6(1-\gamma^2) (2-\gamma^2) \langle J_1 J_2 \rangle \left. \right) \\
& - \frac{1}{6} \left(\gamma (27+36\gamma^2-224\gamma^4+192\gamma^6-48\gamma^8) \langle x^3 \rangle + (108-324\gamma^2+216\gamma^4-48\gamma^6) \langle x^2 J_1 \rangle + 6\gamma(3-2\gamma^2)^3 \langle x q^2 \rangle \right. \\
& \left. - 36\gamma \langle x J_1^2 \rangle - 18\gamma \langle x J_2 \rangle - 8\gamma^2 \langle J_1^3 \rangle - 12\gamma^2 \langle J_1 J_2 \rangle \right) \mathcal{H}_2^+(\nu, \sqrt{1-\gamma^2}) \left. \right]. \tag{9}
\end{aligned}$$

Eqs (5)-(6) (together with the next order expansion available online) are the main theoretical result of this paper.

II. IMPLEMENTATION

Evaluating these estimators requires computing the cumulants appearing in Eqs. (7)-(9). In non-Gaussian models where the field is represented by the functional of a Gaussian field this may be possible directly, while in general, as shown in [6], such cumulants can be found as weighted marginals of the underlying bispectrum, (to third order), trispectrum (to fourth order), *etc.* On a sphere, the high order marginals are particularly cumbersome and time consuming to compute, as they also involve the contractions of $n-j$ Wigner symbols. Here we suggest a different route, based on the assumption that scientists interested in fitting extrema counts to non-Gaussian maps are typically in a position to generate realizations of such maps. In that case, it becomes relatively straightforward to draw samples of such maps, and estimate the corresponding cumulants. The HEALPIX [8] library provides in fact a direct estimate of the derivatives of such maps up to second order, which is all that is required to compute the cumulants of the JPDF.

As an illustration, let us generate sets of parameterized non-Gaussian maps using the package `sky-ng-sim` [9] of HEALPIX. In this so called harmonic model, the PDF of the pixel temperature, T is given by $\exp(-T^2/2\sigma_0^2) |\sum_{i=0}^n \alpha_i C_i H_i(T/\sigma_0)|^2$, where C_i are normalization constants. In this paper, we use `NSIDE=2048`, $\ell_{\max} = 4096$, $n = 2$, $\sigma_0 = 1$, $\alpha_0 = 0$ and vary α_1 and α_2 . We also consider the second option of `sky-ng-sim` which produces non Gaussian field as even power, β of unit variance zero mean Gaussian fields. For each set of maps, we compute its derivatives, and arithmetically average the corresponding cumulants, using a code, `map2cum` relying on the HEALPIX routine `alm2map_der`. Invariant variables J_1 and J_2 on a sphere are defined via the mixed tensor of covariant derivatives $J_1 = x_{;i}{}^i$ and $J_2 = J_1^2 - 4 |x_{;i}{}^{ij}|$. The differential counts are then evaluated for a range of threshold, $\nu \in [-5, 5]$. For each of

these maps, the number of extrema is computed by the procedure `map2ext` which implements the following algorithm: for every pixel a segment of quadratic surface is fit in the tangent plane based on the temperature values at the pixel of origin and its HEALPIX neighbours. The position of the extremum of this quadratic, its height and its Hessian are computed. The extremum is counted into the tally of the type determined by its Hessian if its position falls within the original pixel. Several additional checks are performed to preclude registering extrema in the neighbouring pixels and minimize missing extrema due to jumps in the fit parameters as region shifts to the next pixel. Masks are treated by not considering pixels next to the mask boundary. Pixel-pixel noise covariance can be included while doing the local fit. On noise-free maps the procedure performs with better than 1% accuracy when the map is smoothed with Gaussian filter with FWHM exceeding 6 pixels. Both `map2cum` and `map2ext` are available upon request. Figure 1 illustrates the very good agreement between the theoretical expectation of the differential number counts to the measured ones for both the harmonic and the power-law models.

An alternative numerical procedure, broadly inspired from importance sampling [e.g. 10], which is likely to be more practical for expansion beyond the fourth order was also successfully explored for 2D topological invariants. Starting from Eq. (3), we re-express both the polynomials in J_1, J_2, ζ , and q^2 and G_{2D} in terms of the six field variables, (x, x_i, x_{ij}) . We then construct formally the marginal $G_\nu(\mathbf{x} = (x_{11}, x_{12}, x_{22}) | x = \nu, x_1 = x_2 = 0)$, where the latter condition corresponds to imposing that we are seeking extrema of the field. It becomes straightforward to draw large sets of 3 random numbers satisfying G_ν . For each triplets, \mathbf{x} , and a given numerical set of cumulants, we then compute the argument, $\mathcal{I}(\mathbf{x})$ of the square bracket in Eq. (3) (up to some given order), together with the two eigenvalues of the Hessian. For maxima (resp. minima, resp. saddle points), we replace \mathcal{I} by 0 if the two eigenvalues are not negative (resp. positive, resp. of different sign). The sum over all triplets yields a Monte Carlo estimate of $\partial n_{\text{ext}}/\partial \nu$. The accuracy of the estimate depends on the extent of rejection while

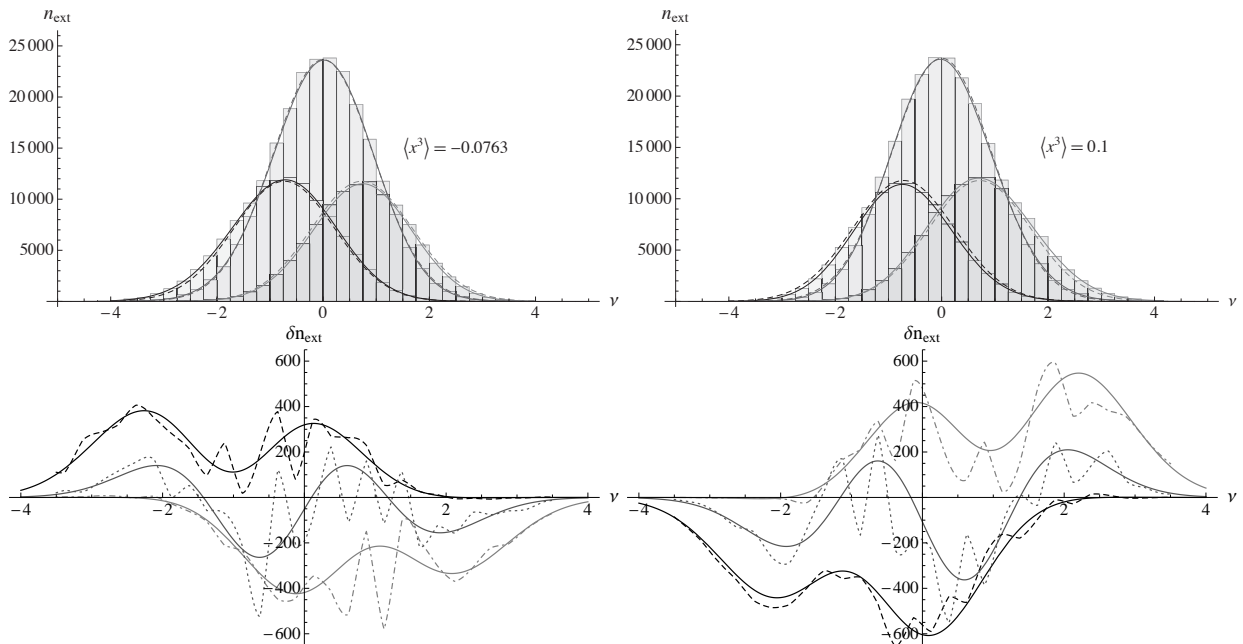


FIG. 1: *Top panel:* the predicted (solid line) number of maxima (right), saddle (middle), and minima (left) in $\Delta\nu = 0.25$ bins as a function of the threshold, ν , on top of the measured count from a *single* realization full-sky $N_{\text{SIDE}}=2048$ HEALPIX map (histogram). The temperature field is smoothed with the Gaussian filter of 10 arcmin FWHM, resulting in $R_* \approx 5.5$ arcmin ≈ 3 pixels. The dashed line corresponds to the Gaussian prediction. The left panel corresponds to the Harmonic Oscillator model of non Gaussianity with $\alpha_1 = 0.6$, $\alpha_2 = 0.6$ (for which $\langle x^3 \rangle = -0.07$), while the right panel corresponds to the power law non Gaussianity with $\beta = 2$ (for which $\langle x^3 \rangle = 0.1$). *Bottom panel:* the departure from Gaussianity for these two models as predicted (solid line) and measured (dashed line) for maxima (light grey), minima (dark grey) and saddle points (grey). Note that the corrections of Eqs (5)-(6) (solid line) give a very accurate match to the measured PDF. As is seen, different models of non-Gaussianity can be distinguished by their effects on extrema.

applying the extremal condition.

Note in closing that all the presented analysis is straightforwardly generalized to 3D (noticeably the Monte Carlo method), as shown in [11], to describe the large scale distribution of matter. Indeed in this context, the gravitational instability that nonlinearly maps the initial Gaussian inhomogeneities in matter density into the LSS, induces strong non-Gaussian features culminating in the formation of collapsed, self-gravitating objects such as galaxies and clusters of galaxies.

Acknowledgments: we warmly thank E. Hivon for his help. CP and DP thanks the department of physics, Oxford, for hospitality during the completion of this work. The Gram-Charlier to cumulants lookup table is available at <http://www.iap.fr/users/pichon/Gram/>, together with the second order extrema counts, and third order genus given by K_1 . All codes to compute the cumulants of given fields and the extrema on the HEALPIX pixelisation are available upon request.

-
- [1] R. J. Adler, *The Geometry of Random Fields* (The Geometry of Random Fields, Chichester: Wiley, 1981).
- [2] A. G. Doroshkevich, *Astrofizika* **6**, 581 (1970).
- [3] J. M. Bardeen, J. R. Bond, N. Kaiser, and A. S. Szalay, *ApJ* **304**, 15 (1986).
- [4] D. Pogosyan, C. Gay, and C. Pichon, *Phys. Rev. D* **80**, 081301 (2009), 0907.1437.
- [5] T. Matsubara, *ApJ* **584**, 1 (2003).
- [6] T. Matsubara, *Phys. Rev. D* **81**, 083505 (2010), 1001.2321.
- [7] M. S. Longuet-Higgins, Royal Society of London Philosophical Transactions Series A **249**, 321 (1957).
- [8] K. M. Górski, E. Hivon, A. J. Banday, B. D. Wandelt, F. K. Hansen, M. Reinecke, and M. Bartelmann, *ApJ* **622**, 759 (2005), arXiv:astro-ph/0409513.
- [9] G. Rocha, M. P. Hobson, S. Smith, P. Ferreira, and A. Challinor, *MNRAS* **357**, 1 (2005).
- [10] W. H. Press, S. A. Teukolsky, W. T. Vetterling, and B. P. Flannery, *Numerical Recipes in C++: The Art of Scientific Computing* (Cambridge University Press, 2002), ISBN 0521750334, URL <http://www.amazon.com/exec/obidos/redirect?tag=citeulike07-20&path=ASIN/0521750334>.
- [11] C. Gay, C. Pichon, and D. Pogosyan, in prep. (2011).
- [12] the field and its derivatives are considered normalized by their correspondent variances $\sigma_0^2 = \langle x^2 \rangle$, $\sigma_1^2 =$

$\langle(\nabla x)^2\rangle, \sigma_2^2 = \langle(\Delta x)^2\rangle$. This implies that in our dimensionless units $\langle x^2\rangle = \langle q^2\rangle = \langle J_1^2\rangle = \langle J_2\rangle = 1$.